Analysis of Pulse Transit Time Derived from Imaging Photoplethysmography and Microwave Sensor-based Ballistocardiography

Mototaka Yoshioka, IEEE member
Industrial Solutions Company,
Panasonic Corporation
Osaka, Japan
yoshioka.mototaka@jp.panasonic.com

Souksakhone Bounyong
Industrial Solutions Company,
Panasonic Corporation
Osaka, Japan
bounyong.souksakhone@jp.panasonic.com

Abstract

We present a basic analysis of the pulse transit time derived from imaging photoplethysmography and ballistocardiography. The pulse transit time is considered as an indicator of blood pressure. For convenient estimation of the blood pressure, previous studies have used the time delay between electrocardiography and photoplethysmography using contact based sensors, which is known as the pulse arrival time. In this paper, we propose a noncontact system to measure the pulse transit time, which consists of microwave and image sensors. The microwave sensor allows ballistocardiography from tiny body movements generated by the human heartbeat using reflected wave signal from a subject's chest, and the image sensor enables imaging photoplethysmography of subject's face. By temporally synchronizing two noncontact sensors, the proposed system is able to provide an estimate of the pulse transit time remotely. We conducted experiments on 16 subjects (age range of 69 to 79 years old) with a supine posture. The correlation coefficient between the noncontact pulse transit time and systolic blood pressure was −0.64 ($P<0.05$). The pulse transit time had a better correlation with systolic blood pressure than the pulse arrival time, which was −0.20. This result indicates that the pre-ejection period influences the pulse arrival time. The pre-ejection period calculated from electrocardiography to ballistocardiography ranges from 54 to 130 ms owing to individual differences. This is an important finding for noncontact blood-pressure estimation in the future.

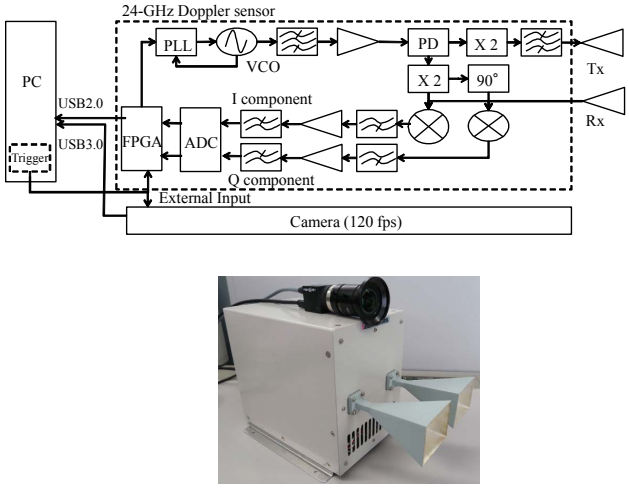

Fig. 1. A block diagram and a photograph of a prototype system for noncontact PTT mesurement. The size of microwave sensor is 13W x 17H x 20L in centimeter.

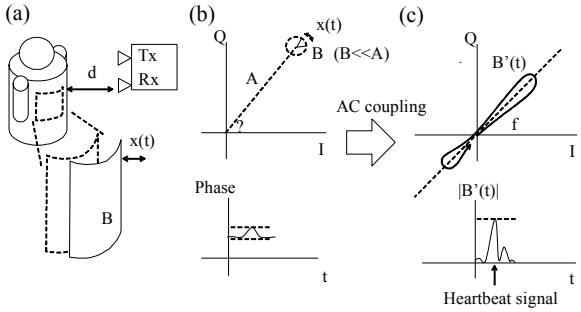

Fig. 2. Illustration of BCG using a microwave sensor.

1. Introduction

Since the early report in 2011 of remote detection of a heartrate signal with prevalent web camera using independent component analysis [1], many studies have focused on improving the robustness and expanding the applications of this technique [2]. In principle, the arrival a pulse to body parts such as the skin surface on the face or palms results in a tiny change of brightness, allowing detection using a camera. To distinguish and extract the pulse signal from noise due to the ambient light signals and motion artifacts, a number of approaches have been conducted [3]-[5]. For example, McDuff *et al.* [3] suppressed noise and extracted the pulse signal, which has a high absorption approximately 550 nm, using the five band camera. Several studies have reported imaging photoplethysmography (iPPG) under motion by applying an

adaptive filter with red and blue channels [4], or using accurate facial tracking and motion spectrum subtraction [5]. Furthermore, for detection in the dark, such as when the subject is asleep, a near-infrared camera-based PPG (using three wavelengths in the range 760–900 nm and an extraction algorithm) was used for motion-durable PPG [6][7]. In addition to iPPG, radar sensor-based ballistocardiography (BCG) has been investigated [8][9].

BCG is tiny body movement generated by the heartbeat and can be used as a surrogate heartbeat signal for noncontact measurement. Radar-based measurements can be used to obtain the ballistocardiograph from the reflected wave from a subject's chest surface because the radar wave penetrates clothes or even a comforter and directly reflects movements caused by heart contraction. Camera and radar sensors can potentially measure the heart rate (HR) accurately even at a distance of 2 m [9].

Noncontact HR and heart rate variability (HRV) are potentially useful for applications such as stress monitoring [10], exercise monitors [11], and driver monitoring [12]. In addition to the HR and HRV, the pulse transit time (PTT) is an important physiological parameter for daily health monitoring of blood pressure and arterial stiffness. The PTT is the time difference for the pulse wave to travel between two arterial body locations. Several studies for cuff-less blood pressure estimation using the PTT have been conducted [13].

In previous studies, the time between the R-peak of electrocardiography (ECG) signal and the pulse arrival in PPG on the fingertip and other body locations has been used for contact-based measurement [13]. However, these conventional measurements of the duration include the pre-ejection period (PEP) and are often called the pulse arrival time (PAT) to distinguish this from the PTT. The PEP is the time between electrical depolarization, which is a QRS-wave on the ECG, and the ejection of blood with mechanical ventricular contraction generated by the ECG. The PEP is therefore the total duration of the electrical and mechanical events prior to ejection. The PAT and PTT have been used interchangeably, because the PEP is insignificant for measurements HR or HRV. In addition, to analyze the PEP and the difference between the PAT and PTT, a dedicated medical cardiac bio-impedance sensor is required, causing a difficulty to researchers for daily health monitoring.

Several studies have reported a correlation between the BP and PAT (including the PEP) [14][15], whereas other reported that the PTT correlates with the BP but the PAT does not [16][17]. Because BP estimation by PTT is generally based on Moens–Korteweg theory, which represents a propagation of blood flow, PEP (which means a delay of actual ejection) might influence the estimation. Martin *et al*. [18] proposed a bathroom weighing scale-like PTT and BP estimation system. For convenient daily

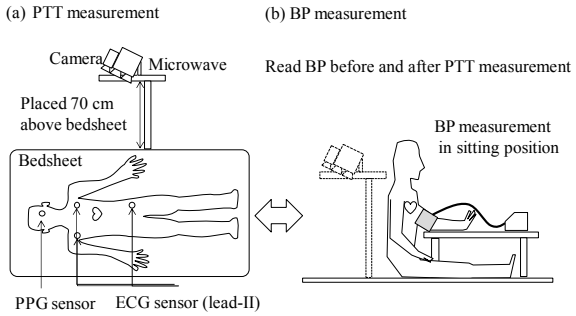

Fig. 3. Experimental setup and protocol.

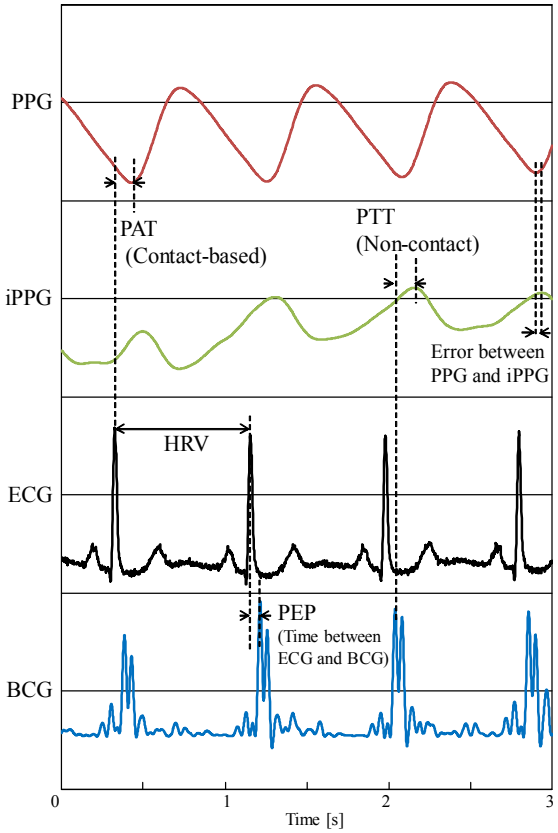

Fig. 4. A subject's reference PPG (red line), iPPG by camera (green line), reference ECG (black line), and BCG by radar (blue line), in order from top to bottom. Note: iPPG is sympetric with PPG. PAT, noncontact PTT, HRV, an error between PPG and iPPG, and PEP are also illustrated.

measurement, the system was composed of a foot PPG sensor and a force plate for recording the BCG, thus yielding the PTT. Furthermore, this study compared the PAT obtained for a reference ECG and PPG, and the proposed PTT, noting superior higher performance of the PTT and better correlation with BP. This demonstrates the potential of this approach for PTT measurement and cuff-less BP.

It is important to continuously measure the PTT while the subject is sleeping for hypertension or morning BP surge. Thus, we present a new approach for non-contact PTT measurement using microwave and image sensors. The microwave sensor is used for BCG, and the image sensor is used for iPPG on image sequences of a subject's face. By temporally synchronizing these sensors, the system is able to obtain the PTT. This system would be suitable to set above a bed to monitor daily vital signs, such as the HRV and PTT.

The paper is structured as follows. Section II illustrates the noncontact PTT measurement system. Section III introduces the experimental condition. Section IV presents the results and the correlation between the BP and contact PAT and noncontact PTT. In Section V, the results and feasibility of PTT are discussed, and Section VI summarizes the study.

2. System Architecture

Figure 1 shows a block diagram of the prototype system. The system is composed of three blocks: a microwave sensor for BCG, a camera for PPG, and a personal computer for temporally synchronizing the two sensor signals and calculating the PTT.

2.1. Doppler Sensor for Ballistocardiography

The microwave sensor consists of a transmitter and transceiver antenna, as shown in Fig. 2(a). The continuous-wave carrier frequency was 24.15 GHz. The sampling rate, output power, and antenna gain were 956 Hz, 1 mW, and 20 dBi, respectively. The sensor conforms to technical standards.

Clutter from the surroundings and immobile target was accumulated as the direct-current (DC) component, which dominates the reflected signal. An alternating-current (AC) coupling module was therefore embedded into the system architecture. The lower cutoff frequency for the AC coupling was adjusted to 5 Hz, which was empirically chosen to suppress not only the DC component but also any respiration effects (which occur at approximately 0.4 Hz) sufficiently while retaining the heartbeat signal. Because the BCG involves tiny modulation of the wave phase, the system was phase-locked to suppress phase distortion and jitter.

The signal $T\cos(2\pi f_0 t)$ with carrier frequency f_0 is transmitted from the microwave sensor, and the transceiver then receives the reflected signal $R\cos(2\pi f_0 t - 4\pi d/\lambda - 4\pi x(t)/\lambda)$ from the subject's chest. Here, d is the distance between the target and sensor, λ is the wavelength, and $x(t)$ is the distance of the subject's chest modulated by BCG. (Fig. 2(a)). The received signal is mixed with the transmitted signal on a mixer and filtered to cut out the high-frequency component. The in-phase (I) and quadrature (Q) components are thus obtained as

$$S_i(t) = V_i + B(t)\cos(\theta - 4\pi x(t)/\lambda), \quad (1)$$

$$S_q(t) = V_q + B(t)\sin(\theta - 4\pi x(t)/\lambda), \quad (2)$$

where V is the DC component and θ is a constant phase associated with the direct waves and the phase delay due to the processing of the mixer.

The heartbeat slightly modulates the amplitude $B(t)$ and phase in proportion to $x(t)$, as shown in Fig. 2(b). The AC coupling applied in this study eliminates the DC component, and the obtained signal is thus

$$S_i(t) = B'(t)\cos(\varphi), \quad (3)$$

$$S_q(t) = B'(t)\sin(\varphi). \quad (4)$$

The BCG is obtained as the trend of the absolute amplitude $|B'(t)|$ (as shown in Fig. 2(c)).

For measurement of the HR or HRV, which have time differences of approximately 700–1000 ms, the phase shift and signal shape due to the filter are often neglected. However, in this study we calculate PTT which is relatively a short period (100–200 ms) by detecting the peak of pulse wave, thus the phase shift cannot be allowed. To prevent phase shift, we applied the finite-impulse-response (FIR) filter and phase compensation to prevent the phase shift [19]. The peaks of $|B'(t)|$ after applying a FIR low-pass filter (empirically determined cutoff frequency of 30 Hz) were detected as the heartbeat timing.

2.2. Image Sensor for Photoplethysmography

An FL3-U3-12S2C-CS camera from Point Grey was used for PPG. The frame rate, resolution of the AD converter, and dynamic range were 120 fps, 12 bits, and 64 dB, respectively, and the captured images were transferred to a personal computer via a USB3.0 connection.

We used OpenCV [20] for face detection, selected the proximate location of the cheek as a region of interest (ROI), and obtain the sequence of the brightness of the green channel as the imaging PPG.

According to conventional studies, the onset of pulse arrivals (which is generally used in PTT calculation) was detected from iPPG. Note that the iPPG signals are inverted from those of contact-based PPG because the pulse absorbs image brightness. Therefore the peaks of iPPG are detected as pulse arrival points. The iPPG peaks were detected after applying a FIR low-pass filter (empirically determined cutoff frequency of 2 Hz) as the pulse arrival point.

2.3. Noncontact Pulse Transit Time Measurement

TABLE I. OBTAINED DATA OF ALL PARTICIPANTS (N = 16)

No.	SBP [mmHg]	DBP [mmHg]	HRV ECG [ms]	HRV PPG [ms]	HRV BCG [ms]	HRV iPPG [ms]	PAT [ms]	PEP [ms]	ME of PPG and iPPG [ms]	PTT [ms]
1	127.0	67.5	1271±10	1270±17	1271±69	1282±78	76 ± 4	54 ± 29	19 ± 28	19 ± 82
2	145.5	85.0	886 ± 16	886 ± 15	884 ± 27	878 ± 115	104 ± 3	74 ± 20	17 ± 86	48 ± 87
3	106.0	58.0	933 ± 13	933 ± 15	982 ± 73	993 ± 113	155 ± 4	104 ±23	54 ± 53	106 ± 61
4	151.5	72.5	1166 ± 7	1166 ± 8	1166 ± 29	1166 ± 75	137 ± 2	107 ±21	8 ± 63	21 ± 62
5	125.5	70.0	943 ± 13	944 ± 15	943 ± 54	942 ± 20	128 ± 3	130 ±33	35 ± 15	33 ± 37
6	113.0	74.5	1033 ± 13	1034 ± 15	1044 ± 98	1090 ± 122	100 ± 4	72 ± 59	66 ± 27	94 ± 70
7	114.5	66.0	1006 ± 66	1006 ± 64	1041±138	1003 ± 101	109 ± 4	72 ± 23	39 ± 42	76 ± 46
8	145.5	78.5	1065 ± 16	1065 ± 17	1070 ± 42	1066 ± 21	111 ± 3	120 ± 16	10 ± 6	13 ± 28
9	143.5	74.0	866 ± 42	866 ± 43	865 ± 71	865 ± 106	132 ± 5	121 ± 34	56 ± 60	58 ± 68
10	115.5	66.0	695 ± 5	695 ± 10	707 ± 52	701 ± 67	124 ± 8	80 ± 27	17 ± 20	26 ± 28
11	121.0	72.5	1084 ± 16	1084 ± 19	1083 ± 30	1093 ± 58	124 ± 5	84 ±16	31 ± 50	71 ± 49
12	131.0	75.0	1195 ± 10	1194 ± 12	1195 ± 19	1205 ± 128	116 ± 3	93 ± 10	13 ± 25	28 ± 28
13	107.5	62.0	1029 ± 6	1028 ± 10	1028 ± 30	1025 ± 19	141 ± 5	61 ± 81	22 ± 20	81 ± 70
14	135.5	79.0	855 ± 20	855 ± 21	853 ± 94	861 ± 69	116 ± 6	119 ± 71	54 ± 45	61 ± 66
15	118.5	76.0	902 ± 45	903 ± 49	897 ± 64	890 ± 71	138 ±13	75 ± 40	27 ± 24	89 ± 41
16	119.0	63.0	867 ± 20	867 ± 21	867 ± 25	867 ± 108	116± 4	59 ± 13	12 ± 83	44 ± 64
Ave.	126 ± 14	71 ± 7	987 ± 143	987 ± 143	987 ± 144	994 ± 145	120 ± 18	89 ± 24	25 ± 24	54 ± 29

Subject number, systoric blood pressure (SBP), diastolic blood pressure (DBP), heartrate variability (HRV) by each sensor, pulse arrival time (PAT), pre-ejection period (PEP) obtained by ECG and BCG, error between PPG and iPPG, and noncontact PTT are shown. SBP and DBP are the average values between before and after PTT measurement. All data is represented as means and standards deviations.

The sequences of microwave and image signals were carefully synchronized using an external trigger generated by a personal computer. An associated mean error of approximately 4 ms during a 20-s measurement interval was confirmed.

Thus, the PTT could be calculated from the time difference between a peak in the BCG data acquired by the microwave sensor and the nearest arrival point of the imaging PPG.

3. Experimental protocol

The experiment was conducted on 16 subjects (ages: 69–79 years; gender: 6 males, 10 females; BMI: 18–24 kg/m^2; and height: 150–176 cm). Informed consent to this experiment was obtained from all subjects. As a reference, contact-based PPG and ECG were recorded using a commercially available biosignal recorder (Polymate V by Miyuki Giken).

ECG was performed with electrodes placed on the subject's chest (lead-II configuration), and the facial PPG was measured by a PPG sensor attached to the subject's cheek (Fig. 3(a)). The sampling rate of both data was 1000 Hz. For temporal consistency with the reference and the system, an electrical trigger was used to synchronize the start and end points.

The PAT and PTT depends on the posture, and relatively stable measurements can be obtained in the recumbent position [13][21]. Therefore, participants were requested to lie on their backs with normal breathing, and to remain still during the measurements for precise data acquisition and analysis.

As shown in Fig. 3(a), both the microwave sensor and camera were placed approximately 70 cm above the bed; the microwave sensor was orientated toward the subject's chest wall and the camera orientated toward the subject's face to capture facial images. The experiments were conducted under ambient light.

The measurement period was approximately 20 s. Systolic blood pressure (SBP) and diastolic blood pressure (DBP) were measured with the subject in the sitting position before and after PTT measurement with an assumption that the average BP is similar to that during the recording. Using a cuff-type sensor of BP (Panasonic, EW-BU35), the subject's left arm was placed on a table so that it was at approximately the same height as the subject's heart (Fig. 3(b)) and the BP was measured.

4. Experimental Results

Table I lists data (mean ± standard deviation) obtained from all subjects. Figure 4 shows an example of the iPPG, BCG, and their reference sequences for one subject. The parameters measured by sensors; HRV, PAT, PEP (time between the peak of the R-wave and BCG), noncontact PTT, and mean error between iPPG and PPG are also illustrated in Fig. 4.

Similar to waveform in Fig. 4, relatively clear signals and peaks were obtained remotely for most subjects because the experiment was conducted under almost-ideal conditions.

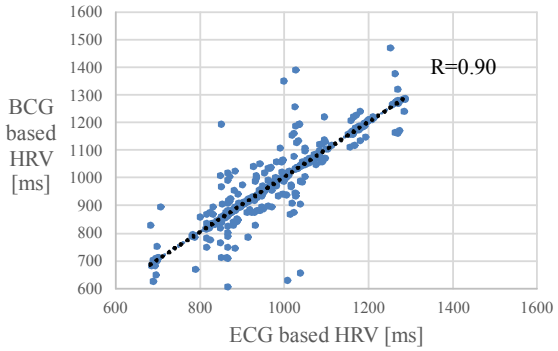

Fig. 5. A scatter plot comparing measurements of ECG based HRV and BCG based HRV [ms].

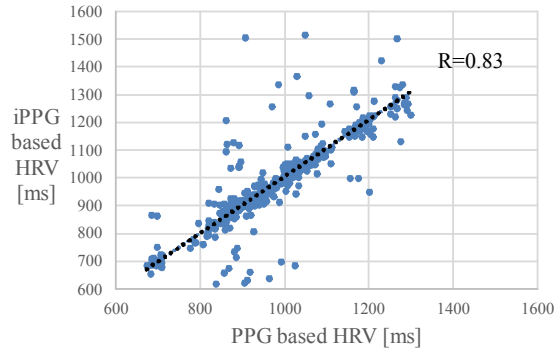

Fig. 6. A scatter plot comparing measurements of PPG based HRV and BCG based HRV [ms].

The BCG and iPPG based HRV was 700–1160 ms, which corresponded closely to the value measured using the reference PPG and ECG. Although the remote detection resulted in some degree of error, the correlation of HRV with ECG (as reference) and BCG from all subjects was 0.90 (Fig. 5), and correlation between PPG and iPPG was 0.83 (Fig. 6). The noncontact PTT calculated from each peak of the iPPG and BCG signals was 13–106 ms in each subject.

The delay between the ECG to BCG caused by the PEP was varied widely from 54 to 130 ms. The PEP has been reported to be variable from approximately 40 to 120 ms with the use of contact-based medical sensors [16]. Thus, the values in our study are reasonable.

Errors between the reference PPG and iPPG were also observed in each subject with the average of 25 ± 24 ms. It was due to the sampling rate of image sensor (120 fps), which is significantly lower than that of the other sensors (1000 Hz), and the weak iPPG signal peaks, which introduced error in peak detection. Thus, further improvement is required in future work.

The correlation of the subject's SBPs and PATs was −0.20 (Fig. 7), the correlation between the SBP and the

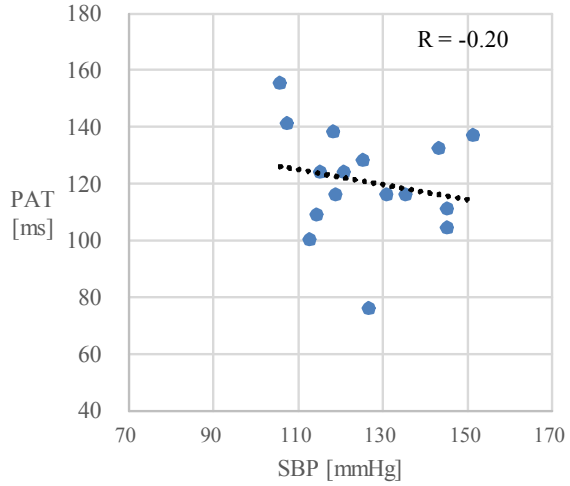

Fig. 7. A scatter plot comparing measurements of SBP [mmHg] and PAT [ms].

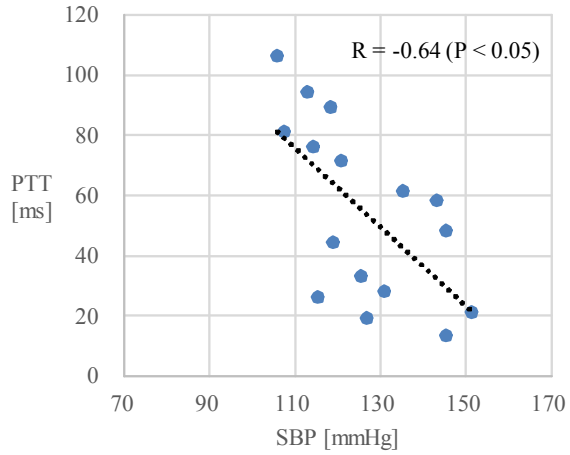

Fig. 8. A scatter plot comparing measurements of SBP [mmHg] and noncontact PTT [ms].

proposed PTT was −0.64 ($P < 0.05$) (Fig. 8). The finding that the BCG-based PTT has better correlation with BP than PAT is consistent with a previous study [18], and indicates that the PTT could be a better indicator for BP than PAT.

5. Discussion

Using remote iPPG and BCG, we obtained the PTT with relatively high accuracy, in part owing to the ideal conditions used. Thus, we cannot definitively conclude that this method is superior to previous methods for daily use. However, this method does enable the measurement of PTT without the effect of PEP, and the resulting PTT is a better indicator of BP than PAT.

Although the correlation coefficient of noncontact PTT

and SBP was −0.64 which is lower than the result in previous study (correlation coefficient of −0.80), this showed a potential of noncontact PTT measurement for blood pressure estimation. The correlation between DBP and PAT was −0.3, and the correlation between DBP and PTT was −0.2, which are significantly lower than when using SBP. This result showed a similar result as reported in the previous studies [22][23].

We note that our observations in elder subjects are similar to those of a previous study conducted with only young subjects (age range of 25–27). This would contributes to future investigation and widely usage of cuff-less BP estimation using BCG based PTT.

The PAT was measured from ECG and PPG sensors attached on subjects' face, which is relatively a short distance. Although the PATs were 76–155 ms, PEPs were observed from 54 to 130 ms, which occupied PATs by considerably a large margin. In addition to individual differences among subjects, this obscured the relationship between the BP and PAT.

The radar-based BCG also includes several delays and distortion because of factors such as the thickness of muscle or fatty layers which causes the inconsistency of peak detection. Although we used the BCG peaks for simplicity, investigation of other parts of the BCG signal is necessary.

Previous studies using PPG for BP estimation reported that it is better to measure the signal at the arrival point of the pulse (i.e., at the foot of the signal) than after the arrival point (i.e., at the peak of the signal). Furthermore, some have reported the first derivative point of the pulse wave is also informative [22][23]. Although we used the peak in the BCG signal to calculate the PTT, the wave foot of the signal would possibly be more informative because this is the point at which the heart starts contracting. Thus, further analysis is needed to achieve the most accurate PTT.

Previous studies reported a PAT of approximately 300–400 ms derived from ECG and PPG from finger tips [24]. This longer time could reduce the influence of PEPs compared with our measurement. However, when the distance is increased, other factors are expected to come into play, such as the conditions of the arteries, the subject's posture. Thus, for noncontact measurement, radar-based BCG and facial PPG is a desirable combination, because we can capture BCG directly from the chest, and because it is more practical to analyze facial images than other body parts.

6. Summary

We proposed a non-contact-based PTT measurement technique using microwave and image sensors. The obtained PTT correlates better with BP than the conventional indicator PAT, indicating the influence of PEP and possibility of indicator for BP estimation. Because we carried out this study on a small sample size (16 human subjects), future studies with a large sample size are needed to conclusively determine the influence of the PEP for PTT-based BP estimation. Improvements in data analysis and better algorithms would allow us to improve the accuracy of peak detection of the microwave and pulse wave from the camera, and thus increase the accuracy of the PTT measurement. For practical use, an IR camera is preferable to an RGB camera because it would allow monitoring of subjects in the dark. Thus, in future work, we will combine an IR camera and microwave to collect long-term data while subjects are sleeping.

References

[1] M. Z. Poh, D. McDuff and R. W. Picard. Advancements in noncontact, multiparameter physiological measurements using a webcam. *IEEE Trans. Biomed. Eng.,* 58(1):7-11, 2011.

[2] D. J. McDuff, J. R. Estepp, A. M. Piasecki and E. B. Blackford. A survey of remote optical photoplethysmographic imaging methods. *2015 37th Annual International Conference of the IEEE Engineering in Medicine and Biology Society (EMBC),* Milan, 2015, pp. 6398-6404.

[3] D. McDuff, S. Gontarek, and R. W. Picard. Improvements in remote cardiopulmonary measurement using a five band digital camera. *IEEE trans. Biomed. Eng.,* 61(10): 2593-2601, 2014.

[4] L. Feng, L. M. Po, X. Xu, Y. Li, and R. Ma. Motion-resistant remote imaging photoplethysmography based on the optical properties of skin. *IEEE Trans. Circuits Syst. Video Technol.,* 25(5):879–891, May 2015.

[5] B.-F. Wu, P.-W. Huang, C.-H. Lin, M.-L. Chung, T.-Y. Tsou, and Y.-L. Wu. Motion resistant image-photoplethysmography based on spectral peak tracking algorithm. *IEEE Access,* 6:21621-21634, Apr. 2018.

[6] M. van Gastel, S. Stuijk, and G. de Haan. Motion robust remote-PPG in infrared. *IEEE Tran. Biomed. Eng.,* 62(5): 1425-1433, Feb. 2015.

[7] W. Wang, A. C. Den Brinker, and G. De Haan. Discriminative signatures for remote-ppg. *IEEE Trans. Biomed. Eng.,* Aug. 2019. doi: 10.1109/TBME.2019.2938564.

[8] I. V. Mikhelson, S. Bakhtiari, T. W. Elmer, and A. V. Sahakian. Remote sensing of heart rate and patterns of respiration on a stationary subject using 94-GHz millimeter-wave interferometry. *IEEE Trans. Biomed. Eng.,* 58(6):1671-1677, 2011.

[9] L. Ren, L. Kong, F. Foroughian, H. Wang, P. Theilmann, and A. E. Fathy. Comparison study of noncontact vital signs detection using a Doppler stepped-frequency continuous-wave radar and camera-based imaging photoplethysmography. *IEEE Trans. Microw. Theory Techn.*, 65(9):3519–3529, Sep. 2017.

[10] D. McDuff, S. Gontarek, and R. W. Picard. Remote measurement of cognitive stress via heart rate variability. *in*

Engineering in Medicine and Biology Society (EMBC), 2014 36th Annual International Conference of the IEEE, IEEE, 2014, pages 2057-2960.

[11] W. Wang, B. Balmaekers, and G. de Haan. Quality metric for camera-based pulse rate monitoring in fitness exercise. *in Proc. IEEE Int. Conf. Image Process. (ICIP), Sep. 2016,* pages 2430–2434.

[12] Z. guo, Z. J. Wang, and Z. Shen. Physiological parameter monitoring of drivers based on video data and independent vector analysis. *IEEE International Conference on Acoustic, Speech and Signal Processing (ICASSP),* pages 4374-4378, 2014.

[13] R. Mukkamala, J.-O. Hahn, O. T. Inan, L. K. Mestha, C.-S. Kim, H. Töreyin, and S. Kyal. Toward ubiquitous blood pressure monitoring via pulse transit time: theory and practice. *IEEE Trans. Biomed. Eng.,* 62(8):1879–1901, Aug. 2015.

[14] H. Gesche, D. Grosskurth, G. Kuchler, and A. Patzak. Continuous blood pressure measurement by using the pulse transit time: comparison to a cuff-based method. *Eur. J. Appl. Physiol,* 112(1):309-315, 2012.

[15] M. Kachuee, M. M. Kiani, H. Mohammadzade, and M. Shabany. Cuffless Blood Pressure Estimation Algorithms for Continuous Health-Care Monitoring. *IEEE Trans. Biomed. Eng,* 64(4):859-869, 2017.

[16] R. A. Payne, C. N. Symeonides, D. J. Webb, and S. R. J. Maxwell. Pulse transit time measured from the ECG: An unreliable marker of beat-to-beat blood pressure. *J. Appl. Physiol.*, 100(1):136–141, 2005.

[17] G. Zhang, D. Xu, N. B. Olivier, and R. Mukkamala. Pulse arrival time is not an adequate surrogate for pulse transit time in terms of tracking diastolic pressure. *2011 Annual International Conference of the IEEE Engineering in Medicine and Biology Society (EMBC),* Boston, MA, 2011, pages 6462-6464.

[18] S. L.-O. Martin, A. M. Carek, C. -S. Kim, H. Ashouri, O. T. Inan, J. O. Hahn, R. Mukkamala. Weighing scale-based pulse transit time is a superior marker of blood pressure than conventional pulse arrival time. *Scientific reports,* 6:39273, 2016.

[19] M. Yoshioka, K. Murakami, and J. Ozawa. Improved human pulse peak estimation using derivative features for noncontact pulse transit time measurements. *2015 International Joint Conference on Neural Networks (IJCNN),* 2015, pages 1-6.

[20] https://opencv.org/

[21] L. Yan, S. Yin, S. Wang, J. Liu, L. Xu, and Y. Zhao. Study on the variability of pulse wave and ECG of graduate students with different body positions. *Proceeding of the IEEE International Conference on Information and Automation*, pages 658-662, 2012.

[22] Y. Liang, D. Abbott, N. Howard, K. Lim, R. Ward, and M. Elgendi. How effective is pulse arrival time for evaluating blood pressure? Challenges and recommendations from a study using the MIMIC database. *Journal of clinical medicine*, 8(3):337, 2019.

[23] Y. Z. Yoon, J. M. Kang, Y. Kwon, S. Park, S. Noh, Y. Kim, J. Park, and S. W. Hwang. Cuff-less blood pressure estimation using pulse waveform analysis and pulse arrival time. *IEEE journal of biomedical and health informatics*, 22(4):1068-1074, 2017.

[24] S. Rajala, T. Ahmaniemi, H. Lindholm, and T. Taipalus. Pulse arrival time (PAT) measurement based on arm ECG and finger PPG signals - comparison of PPG feature detection methods for pat calculation. *2017 39th Annual International Conference of the IEEE Engineering in Medicine and Biology Society (EMBC), July 2017,* pages 250-253.